CHEMISTRY OF MATERIALS
Article

Chem. Mater. **2010,** *22,* 241–246 241
DOI:10.1021/cm902918a

Polyelectrolyte-Mediated Electrochemical Fabrication of a Polyacetylene p−n Junction

Stephen G. Robinson,[†] Dean H. Johnston,[‡] Christopher D. Weber,[†] and Mark C. Lonergan*,[†]

[†]*Department of Chemistry and The Materials Science Institute, University of Oregon, Eugene, Oregon, 97403 and* [‡]*Department of Chemistry, Otterbein College, Westerville, Ohio, 43801*

Received September 18, 2009. Revised Manuscript Received November 6, 2009

The diffusion of dopant counterions has made the formation of conjugated polymer p−n junctions challenging. We demonstrate polyelectrolyte mediated electrochemistry (PMEC) as a three-electrode technique for separately introducing n- and p-type regions in an ion-functionalized polyacetylene structure to form a p−n junction. PMEC uses a polyelectrolyte-based supporting electrolyte and ion-functionalized conjugated polymers to control the ions available for exchange between a solid sample and supporting electrolyte, and in this way, select for oxidative vs reductive electrochemical processes. A bilayer consisting of solid layers of anionically and cationically functionalized polyacetylenes was driven first to −1.5 V vs SCE and then to 0.6 V vs SCE using tetrabutylammonium polystyrene sulfonate/acetonitrile as a supporting electrolyte. The negative potential step n-doped the entire structure, and the positive potential step selectively p-doped the anionically functionalized layer to form a p−n junction as followed by spectroelectrochemistry and supported by current−voltage characterization. The polyacetylene p−n junctions were observed to exhibit diode behavior with ideality factors in the range of 3−3.5. Rectification ratios of greater than 500 at 1 V were achieved, and the junctions exhibited a small photovoltaic effect.

Introduction

Junctions such as the p−n junction where a discontinuity exists in dopant type or density are ubiquitous in silicon-based electronics,[1] but examples of such junctions are far less common with conjugated polymers. One important reason is the instability created by the mobile dopant ions that are typically present in doped conjugated polymers. In the case of a p−n junction, for instance, any diffusible dopant ions will support a bulk redox reaction between the n- and p-type regions that destroys the junction (reverse reaction of Figure 1A).[2]

A number of trapping approaches have been developed to overcome the problem of dopant-ion diffusion. These approaches rely on the application of an electrical bias across an ion-containing sample to drive redox disproportionation, thus forming n- and p-type regions at the electrodes (forward reaction in Figure 1A). The otherwise transient junction is then trapped by reducing the temperature to freeze out the ions,[3−6] by using ion-pair monomers that are polymerized to reduce their mobility,[7,8] or by using ion-functionalized conjugated polymers (conjugated ionomers[9,10] or conjugated polyelectrolytes[11]), which allow the ions liberated in the disproportionation step to be removed by solvent washing (forward reaction of Figure 1B).[12] A key limitation of the above trapping approaches is that the doping of the two regions is coupled because they are two-electrode techniques. Oxidation at one electrode to form the p-type region is coupled to reduction at the other electrode to form the n-type region. Methods by which the n- and p-doped regions are created independently would provide for the creation of structures that are not possible with current trapping approaches. The goal of this paper is to demonstrate polyelectrolyte-mediated electrochemistry (PMEC) as a three-electrode method for separately introducing n- and p-type regions in the fabrication of a conjugated polymer p−n junction.

*Author to whom correspondence should be addressed. E-mail: lonergan@uoregon.edu.

(1) Sze, S. M. *Semiconductor Devices Physics and Technology* 2nd ed.; Wiley: New York, 2002.
(2) Buck, R. P.; Surridge, N. A.; Murray, R. W. *J. Electrochem. Soc.* **1992**, *139*, 136–144.
(3) Gao, J.; Yu, G.; Heeger, A. J. *Appl. Phys. Lett.* **1997**, *71*, 1293–1295.
(4) Gao, J.; Li, Y.; Yu, G.; Heeger, A. J. *J. Appl. Phys.* **1999**, *86*, 4594–4599.
(5) Yu, G.; Cao, Y.; Andersson, M.; Gao, J.; Heeger, A. J. *Adv. Mater.* **1998**, *10*, 385–388.
(6) Shin, J. H.; Xiao, S.; Fransson, A.; Edman, L. *Appl. Phys. Lett.* **2005**, *87*, 043506/1–043506/3.
(7) Leger, J. M.; Rodovsky, D. B.; Bartholomew, G. P. *Adv. Mater.* **2006**, *18*, 3130–3134.
(8) Leger, J. M.; Patel, D. G.; Rodovsky, D. B.; Bartholomew, G. P. *Adv. Funct. Mater* **2007**, *18*, 1212–1219.
(9) Nguyen, T. Q.; Schwartz, B. J. *J. Chem. Phys.* **2002**, *116*, 8198–8208.
(10) Langsdorf, B. L.; Zhou, X.; Adler, D. H.; Lonergan, M. C. *Macromolecules* **1999**, *32*, 2796–2798.
(11) Jiang, H.; Taranekar, P.; Reynolds, J. R.; Schanze, K. S. *Angew. Chem., Int. Ed.* **2009**, *48*, 4300–4316.
(12) Cheng, C. H. W.; Lonergan, M. C. *J. Am. Chem. Soc.* **2004**, *126*, 10536–10537.

Published on Web 12/14/2009

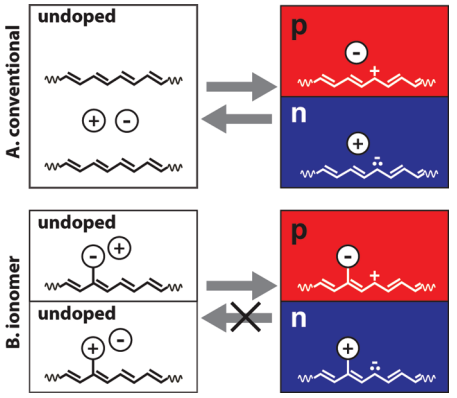

Figure 1. (A) Schematic for the doping (forward reaction) of a conventional conjugated polymer with dissolved salt to form a conjugated polymer p−n junction and undoping (reverse reaction) of a conjugated polymer p−n junction to form an undoped polymer and salt. The reverse reaction illustrates the instability of conjugated polymer p−n junctions containing mobile dopant counterions. The forward reaction can be achieved, for example, by applying an electrical bias across the sample to drive redox disproportionation, but without a means of altering the mobility of the ions after doping, the resulting junction is unstable with respect to redox comproportionation (reverse reaction) after removal of the bias. (B) Schematic for the doping (forward reaction) of a bilayer structure consisting of anionic and cationic ion-functionalized conjugated polymers, with the loss of exchangeable ions, to form a conjugated polymer p−n junction. The resulting p−n junction is stabilized with respect to the reverse reaction because the dopant counterions are covalently bound to the polymer backbone.

In the PMEC approach, doping is controlled by manipulating the counterions available to support electrochemical doping. The availability of counterions is controlled by using a combination of ion-functionalized conjugated polymers with different signs of exchangeable counterions *and* a supporting electrolyte based on a large polymeric ion. Elliott and co-workers showed in the context of redox polymer films that the electrochemistry of a solid film can be controlled by using a polyelectrolyte-based supporting electrolyte.[13] In their work, redox processes that required the incorporation of the polymeric ion for charge compensation were suppressed. In the electrochemical doping of a structure to form a p−n junction, the key is not simply to suppress all redox processes of one type (oxidation or reduction), but rather, to selectively oxidize or reduce certain regions. Herein, we demonstrate that this selective redox chemistry is possible by exploiting a combination of a polyelectrolyte-based supporting electrolyte and ion-functionalized conjugated polymers to fabricate a p−n junction. By building ions into the redox active solid film (i.e., using ion-functionalized conjugated polymers), redox processes that would otherwise be inhibited by the polyelectrolyte-based supporting electrolyte can be selectively restored.

Implicit to the PMEC approach is that the resulting p−n junction will be stabilized against reaction between the n- and p-type regions because it is based on ion-functionalized conjugated polymers and designed to yield internally compensated doped forms. Internal compensation refers to the situation where the charge on the polymer backbone is compensated by counterions covalently bound to the polymer backbone.[14,15] Such covalently bound dopant ions are expected to have low mobility and hence be unable to support redox comproportionation of the p−n junction back to the undoped state (reverse reaction in Figure 1B).

Experimental Methods

Materials. Chloroform was distilled from P_2O_5. Methanol was distilled from Mg/iodine. Anhydrous dimethylformamide (DMF) was used as received. Acetonitrile (ACN) was doubly distilled from P_2O_5. Solvents were degassed using three freeze−pump−thaw cycles. Tetrabutylammonium polystyrene sulfonate (Bu_4NPSS) was synthesized by neutralizing polystyrene sulfonic acid (MW 70 000, Polysciences) with tetrabutylammonium hydroxide (Aldrich) and then dialyzing for four days using Spectra/Por 4 cellulose dialysis membranes. The resulting salt was dried in vacuo for 5 days at 80 °C. Tetramethylammonium tetrafluoroborate ($TMABF_4$)(Aldrich) was recrystallized from water and dried in vacuo at 80 °C for 5 days. The anionic polymer (PA_A) was synthesized using ring-opening metathesis polymerization from tetramethylammonium β-cyclooctatetraenylethyl sulfonate as reported previously.[10] The cationic copolymer (PA_C) was synthesized from trimethylsilylcyclooctatetraene and (2-cyclooctatetraenylethyl) trimethylammonium triflate as previously described.[16] The resulting copolymer had a ratio of 7.7:1 trimethylsilyl (TMS) to trimethylammonium functional groups as determined by NMR. The tungsten alkylidene catalyst [W = CH(o-C_6H_4OMe)(NC_6H_5)-[$OCCH_3(CF_3)_2]_2$(THF)] used in the polymerizations was synthesized as described previously.[17]

Device Fabrication. Junctions were fabricated from sandwich structures consisting of a bilayer containing thin films of PA_C and PA_A sandwiched between gold electrodes. These bilayers were formed by spin coating first a DMF PA_C solution (5 μL, 20 mg/mL) followed by a methanol PA_A solution (10 μL, 20 mg/mL) onto a semitransparent Au/Cr (15 nm, 1.5 nm) film electrode on a glass slide. The PA_C layer is insoluble in methanol which prevents dissolution when the PA_A layer is placed on top. The thickness of the individual layers using this approach could be varied from 150 to 600 nm. The actual thickness of each layer was measured using a Dektak 6 M stylus surface profilometer. The bilayer was carefully cleaned back to the electrode edge and a top porous Au electrode[18] (15 nm) was then deposited by thermal evaporation over a portion of the bilayer. For optical absorption experiments, the bottom electrode was omitted because the pair of electrodes created strong interference effects that complicated interpretation of the absorption spectra.

P−N Junction Formation. The bilayer films were soaked for 5 min in ACN (1 mL) under a nitrogen environment. Bu_4NPSS/ACN (0.1M, 1.5 mL) was then added to the ACN. Owing to some solubility of the PA_A layer in Bu_4NPSS/CH_3CN, the bilayer was initially cycled to positive potentials. This positive cycling

(13) Elliott, C. M.; Redepenning, J. G.; Balk, E. M. *J. Am. Chem. Soc.* **1985**, *107*, 8302–8304.
(14) Bauerle, P.; Gaudl, K. U.; Wurthner, F.; Sariciftci, N. S.; Neugebauer, H.; Mehring, M.; Zhong, C. J.; Doblhofer, K. *Adv. Mater.* **1990**, *2*, 490–494.
(15) Freund, M. S.; Deore, B. *Self-Doped Conducting Polymers*; Wiley: Hoboken, NJ., 2007.
(16) Gao, L.; Johnston, D.; Lonergan, M. C. *Macromolecules* **2008**, *41*, 4071–4080.
(17) Johnson, L. K.; Virgil, S. C.; Grubbs, R. H.; Ziller, J. W. *J. Am. Chem. Soc.* **1990**, *112*, 5384–5385.
(18) Dalton, E. F.; Surridge, N. A.; Jernigan, J. C.; Wilbourn, K. O.; Facci, J. S.; Murray, R. W. *Chem. Phys.* **1990**, *141*, 143–157.

rendered the PA_A layer insoluble presumably due to some small degree of cross-linking reactions. The bilayer was doped by first applying a negative potential step to −1.5 V vs SCE for 60s. The sample was then held at open circuit for approximately 30s followed by applying a positive potential step of 0.6 V vs SCE for 60s. The solvent was removed, and the sample washed with ACN (3 × 5 mL), dried under N_2 for 5 min and then dried under vacuum for 12 h before characterization.

Instrumentation and Characterization. Electrochemical doping was performed with a Cypress 66-CS1200 potentiostat using a standard three-electrode cell with a coiled platinum wire counter electrode and a nonaqueous Ag (s) /Ag^+ reference electrode. The reference electrode was prepared from a 3 mm diameter glass tube with a Vycor frit (Bioanalytical Systems, Inc.), filled with 0.075 M $TMABF_4$/0.005 $AgNO_3$/ACN, and it was calibrated with a commercial saturated calomel electrode. Spectroelectrochemistry was performed using an Ocean Optics USB 2000 diode array spectrometer connected via a fiber optic cable. Spectra were referenced against blanks prepared identically to the sample structures but without the polymer layers. Current−voltage experiments on the dried bilayers were performed using an Agilent 4156C semiconductor parameter analyzer. Photoresponse measurements were performed using 50 mW illumination from a focused tungsten-halogen EHJ white light source and the parameter analyzer. EQCM measurements were performed using a Stanford Research QCM100 with AT-cut, 5 MHz, Au/Ti crystals. The resonant frequency was monitored via a Tektronix TM5003 frequency counter interfaced with the QCM control module. Simultaneous voltammetry measurements were conducted using a Solartron 1287. Measurements were carried out in a custom designed cell under an atmosphere of dry N_2. The EQCM measurements were conducted using a Pt counter electrode, Ag wire pseudo reference, and a grounded working electrode.

Results and Discussion

The PMEC approach to fabricating a conjugated polymer p−n junction was demonstrated using ion-functionalized polyacetylenes. The undoped bilayer structure shown in Figure 2A was used as the starting point. The bilayer was fabricated from anionic (PA_A) and cationic (PA_C) polyacetylenes with differing ion densities. Specifically, the ionic functional group densities of PA_A and PA_C were 1 per 4 and 1 per 30 double bonds, respectively. This difference was intentional so as to demonstrate the ability of PMEC to create structures not possible using trapping approaches. Note that the structure of PA_C also incorporates trimethylsilyl (TMS) functional groups for solubility. The bilayer shown in Figure 2 consists of a ∼450 nm thick film of PA_A and a ∼350 nm thick film of PA_C.

Junctions were fabricated using two sequential potential steps applied to the top porous electrode[18] (in contact with PA_A) of the undoped bilayer of Figure 2A and using the supporting electrolyte tetrabutylammonium polystyrenesulfonate (Bu_4NPSS)/CH_3CN. The two steps that were used are Step I: a 60 s potential step to −1.5 V vs SCE; Step II: a 60 s potential step to 0.6 V vs SCE. The −1.5 and 0.6 V vs SCE potentials are sufficient to either n- or p-dope, respectively, single layer films in a conventional electrolyte.[16] It is noted that the doping chemistry is also affected by Donnan equilibria[19] that influence the potential driving force required for doping, as we have previously studied in single layer films of polyacetylene ionomers.[20]

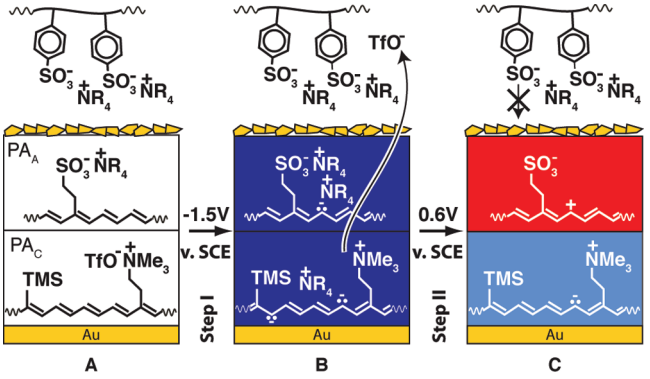

Figure 2. Schematic of the PMEC fabrication of a polyacetylene-based p−n junction using a Bu_4NPSS/CH_3CN supporting electrolyte. (A) Initial undoped bilayer of solid films of a polyacetylene anionomer (PA_A) and a polyacetylene cationomer (PA_C) sandwiched between gold electrodes (the top electrode in contact with PA_A is sufficiently thin so as to remain porous). (B) Structure following the application of −1.5 V vs SCE to the top porous electode to n-dope the films. (C) Structure following the application of 0.6 V vs SCE to the top porous electrode to p-dope the PA_A layer while preserving the PA_C layer in an IC n-type form. Complete reoxidation and p-doping of the PA_C layer is not possible because the original OTf^- anions were previously lost to the solution and PSS^- is too large to permeate the polymer film.

Our idealized picture of how the above potential step sequence yields a p−n junction is as follows. Step I n-dopes the structure as shown in Figure 2B. The reduction of PA_A is supported by the incorporation of R_4N^+ ions from the electrolyte. The reduction of PA_C is supported by both such incorporation and the loss of triflate (OTf^-) anions. The result of oxidative Step II is shown in Figure 2C. As in conventional electrochemistry, the PA_A layer is oxidized first back to its undoped state and then to its p-type state, all supported by the expulsion of R_4N^+ ions. The reoxidation of PA_C, however, cannot fully occur. During Step I, the OTf^- anions are stripped from PA_C and lost to the electrolyte solution, much like in metal stripping. Consequently, the OTf^- anions are not available, and the PSS^- anion is too large to support the complete reoxidation of the n-type PA_C. A component of the n-type doping balanced by the loss of OTf^- anions remains, forming an internally compensated (IC) state where the density of injected charge is balanced by the covalently attached cations. The result is the selective p-doping of the PA_A layer while the PA_C layer remains n-doped.

The formation of a p−n junction was demonstrated by current density−voltage (J-V_{app}) characterization. All of the J-V_{app} data reported were collected on structures that were washed and then dried following electrochemical manipulation, and the bias was applied PA_A vs PA_C. As shown in Figure 3a, diode behavior was clearly observed

(19) Doblhofer, K.; Rajeshwar, K. In *Handbook of Conducting Polymers*, 2nd ed.; Skotheim, T. A., Elsenbaumer, R. L., Reynolds, J. R., Eds.; Marcel Dekker: New York, 1998; pp 531−588.
(20) Lonergan, M. C.; Cheng, C. H.; Langsdorf, B. L.; Zhou, X. *J. Am. Chem. Soc.* **2002**, *124*, 691–701.

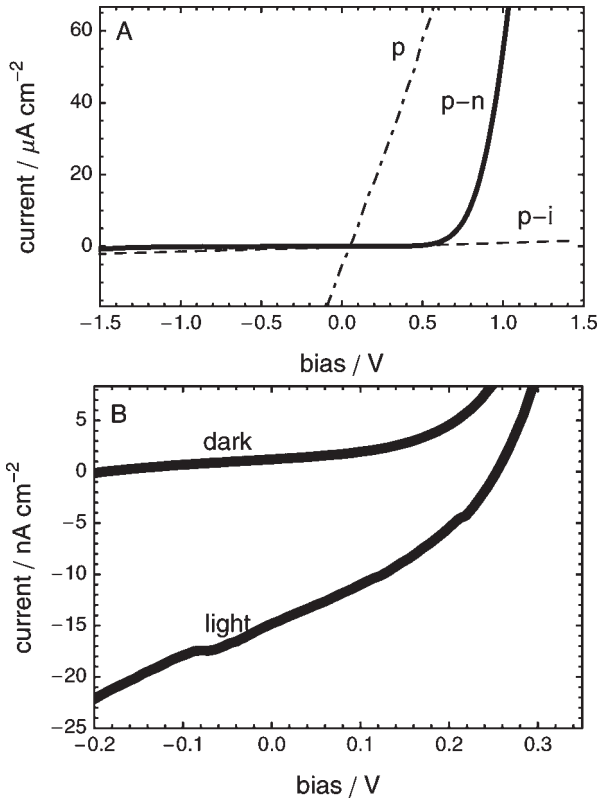

Figure 3. (A) Current density (J)-applied bias (V_{app}) behavior of dry PA_C/PA_A bilayers after the two step doping sequence illustrated in Figure 1 to form a p−n junction (solid line); Control 1 consisting of only Step II (0.6 V vs SCE in Bu_4NPSS/CH_3CN) to form a p−i junction (dashed line); and Control 2 consisting of the same two-step doping sequence used to form the p−n junction but substituting $TMABF_4/CH_3CN$ as the electrolyte to form two p-doped layers (dot-dashed line). (B) Comparison of the J-V_{app} behavior for the same p−n junction as in part A in the dark and under illumination. The film thickness for the PA_A and PA_C layers were ~450 nm and ~350 nm thick, respectively.

(solid line). Consistent with classic p−n junction theory,[1] much greater current was observed for positive bias. The J-V_{app} characteristics did not substantially depend on scan rate at least up to 100 V s^{-1}.

Figure 3 also shows the results of two control experiments. The dashed line shows the J-V_{app} behavior for Control 1: a bilayer subjected to only a positive potential step of 0.6 V vs SCE in Bu_4NPSS (Step II). The Control 1 sample was observed to be much less conductive than the junction subjected to the two-step electrochemical sequence, consistent with oxidation of PA_A while preserving PA_C in its undoped or intrinsic (i) state to form a p−i junction. The PA_C remained undoped in the Control 1 sample and hence poorly conductive presumably because the PSS^- anion is too large to permeate the solid polymer film as would be required to p-dope PA_C. The dot-dashed line shows the J-V_{app} behavior for Control 2: a bilayer subjected to the two-step electrochemical sequence used for p−n junction formation but in the conventional electrolyte tetramethylammonium tetrafluoroborate ($TMABF_4$) rather than in Bu_4NPSS. The Control 2 sample was observed to become conductive and exhibit a linear J-V_{app} relationship. The observed linearity is consistent with both layers becoming p-doped rather than p−n junction formation. Figure 3B expands the J-V_{app} curve and

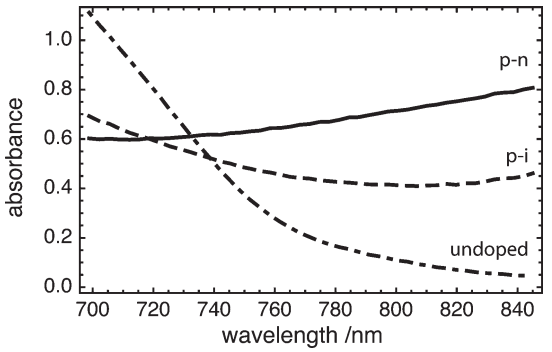

Figure 4. Absorption spectra of a 160 nm PA_C/300 nm PA_A bilayer in its undoped form (dot-dashed line); after only Step II (0.6 V vs SCE in Bu_4NPSS/CH_3CN) to form a p−i junction (dashed line); and after the two step doping sequence illustrated in Figure 1 to form a p−n junction (solid line).

compares it to that under 50 mW illumination from a focused, tungsten-halogen, white light source. A photovoltaic effect, albeit small, was observed consistent with p−n junction formation.

Spectroelectrochemistry was also used to support p−n junction formation. An undoped bilayer was first subjected to a 60 s potential step at 0.6 V vs SCE in Bu_4NPSS/CH_3CN (Step II) to provide an important reference point for later comparison. As discussed and supported with the J-V_{app} data of Control 1, this initial potential step selectively oxidizes the PA_A layer to its p-doped state while leaving the PA_C undoped to from a p−i junction. Figure 4 compares the absorption spectrum of the p−i junction (dashed line) with that of the undoped bilayer (dot−dashed line). As is characteristic for either the n- or p-doping of PA, the p−i junction exhibits a decrease in absorbance on the short wavelength side of the region shown (due to a bleach of the $\pi-\pi^*$absorbance with λ_{max} = 600 nm) and an increase in absorbance on the long wavelength side (due to the tail of the broad NIR absorbance of the doped state with λ_{max} = ~1300 nm) relative to the undoped bilayer. The same bilayer that was used to fabricate the p−i reference junction was then subjected to the two-step sequence described above for p−n junction formation. The spectrum of the resulting structure is shown in Figure 4 (solid line), and it reveals a higher level of doping than observed in the p−i reference. The difference between the spectra assigned to the p−i and p−n junctions illustrate that there is a memory of Step I in the latter case. This memory and the higher degree of doping are consistent with the PA_C layer remaining n-doped during Step II to form the p−n junction.

The assertion that the internally compensated n-type state of the PA_C layer does not undope in Bu_4NPSS/CH_3CN when driven to potentials that would undope or even p-dope PA_C in a conventional electrolyte is key to the formation of the p−n junction. That this is the case was demonstrated by spectroelectrochemical and electrochemical quartz crystal microbalance (EQCM) experiments on single layer PA_C films. Figure 5 shows the absorbance at 800 nm of a single layer PA_C film on a gold electrode while being subjected to the two-step

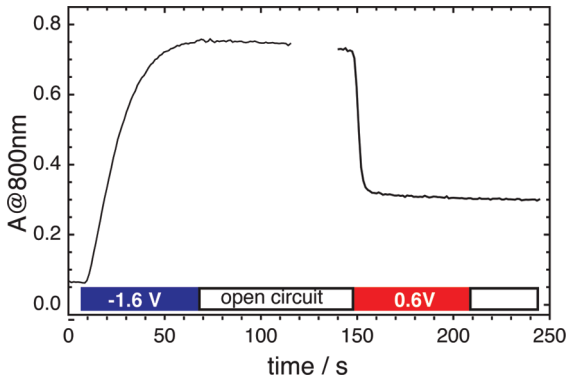

Figure 5. UV−vis absorption changes at 800 nm of a 250 nm thick PA_C monolayer cycled through the two-step doping process used for p−n junction formation. The bar at the bottom edge of the graph shows the potential vs SCE at which the polymer was held during the experiment; the open regions indicate open circuit. The gap in the data is during a period when the software controlling the instruments was being reconfigured for the second potential step. During this gap, the cell was held at open circuit.

doping protocol used to create the p−n junction, although with a slightly more negative Step I potential. The single layer PA_C film was first allowed to sit for 5 s to measure the undoped absorbance. A potential step of −1.6 V vs SCE was then applied for 60s. During the −1.6 V vs SCE potential step, the absorbance at 800 nm was observed to increase and then level off. The observed increase corresponds to n-doping of the sample presumably with the loss of triflate anions and the incorporation of mobile cations from the electrolyte. After the potential step had finished, the sample was monitored at open circuit for 80s. A potential step of 0.6 V vs SCE was then applied, and a drop in the absorbance was observed. The absorbance did not, however, return to its undoped value, but rather leveled off at an absorbance above the undoped state. This persistent absorbance supports the assertion that the film remains n-doped due to the formation of the internally compensated n-doped state of the PA_C. The persistent absorbance is not due to the film becoming p-doped, as if this were the case, the absorbance would be expected to drop to near that of the undoped film and then increase again due to p-doping.

Figure 6 shows EQCM results for a single layer film of PA_C deposited on a gold-coated quartz crystal cycled through n-doping potentials and then through positive p-doping potentials. In the EQCM experiment, voltammetry data (current vs electrode potential E) are collected simultaneously with changes in the resonant frequency (Δf) of the quartz crystal substrate as reflected by the content of Figure 6. In the simplest case, the Δf is sensitive to mass changes in the film with a positive frequency shift corresponding to mass loss. The voltammetry data in Figure 6 show a clear n-doping wave. The Δf upon sweeping to negative potentials and passing through this doping wave shows first a mass loss (positive frequency shift) and then a mass gain (negative frequency shift). The initial mass loss is consistent with doping supported first by the loss of triflate anions from the film, and the subsequent mass increase is consistent with further doping supported by the incorporation of cations from the

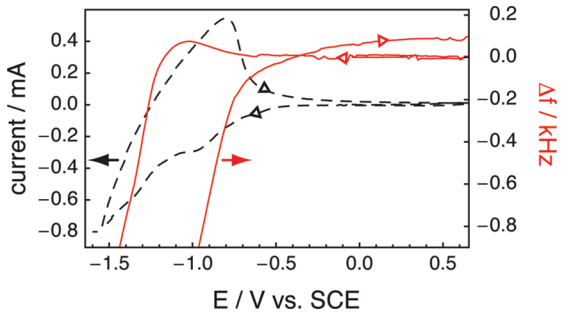

Figure 6. EQCM results collected in 0.1 M Bu_4NPSS/CH_3CN at a scan rate of 30 mV/s for a 250 nm thick film of PA_C. The dotted black line shows the cyclic voltammogram (left axis), and the solid red line shows the change in the resonant frequency (Δf, right axis) of the quartz crystal. The hollow triangles indicate the scan direction. The quartz crystal data are truncated to more clearly show the offset between the initial and final Δf. The ratio of the maximum frequency gain to the maximum frequency loss during the cycle was observed to be 1:16.

electrolyte. Upon reversal of the potential sweep, the Δf trace does not return to its original value, but rather, it returns to the positive frequency maximum that occurred during initial n-doping. This positive difference is consistent with OTf^- anions being lost to the solution during n-doping and hence not being able to support the complete reoxidation to the undoped form. Those OTf^- anions that left the film during n-doping and that had sufficient opportunity to diffuse away from the electrode are not available to support the complete reoxidation of the film, and it remains partially n-doped. Analysis of the voltammetry data also supports the assertion that the polymer film remains n-doped as was previously reported.[20] A notable aspect is the complete absence of a p-doping wave, which would be clearly observed in the potential range studied had a conventional electrolyte been employed. It is noted that the interpretation of EQCM data can be clouded by viscoelastic effects.[21] Although these cannot be completely ruled out, our previous EQCM studies on related ion-functionalized polyacetylenes show a good correspondence between Coulometry and quartz crystal data in Bu_4NPSS/CH_3CN consistent with minimal contributions from viscoelastic effects.[20]

Figure 7 compares a semilogarithmic representation of the J-V_{app} behavior of the PMEC fabricated p−n junction of Figure 3 to two other similarly fabricated junctions. The semilogarithmic representation reveals more detail about the J-V_{app} behavior than the linear representation of Figure 3. For an ideal diode, J is expected to increase exponentially with applied bias for $\beta V_{app} > 3$, where $\beta = q / (kT)$ in so-called strong forward bias, and J is expected to be a constant for $\beta V_{app} < -3$ in so-called strong reverse bias. The slope of the $\log(J) - V_{app}$ curve in strong forward bias is characterized by the ideality or quality factor $n \equiv \beta[d\ln(J)/dV_{app})]^{-1}$ with the minimum value of $n = 1$ indicating the strongest possible dependence of J on V_{app}. The solid line in Figure 7 is a fit to the data in the strong forward bias range of $0.35 < V_{app} < 0.75$ V for the same diode as in Figure 3, and it is

(21) Buttry, D. A.; Ward, M. D. *Chem. Rev.* **1992**, *92*, 1355–1379.

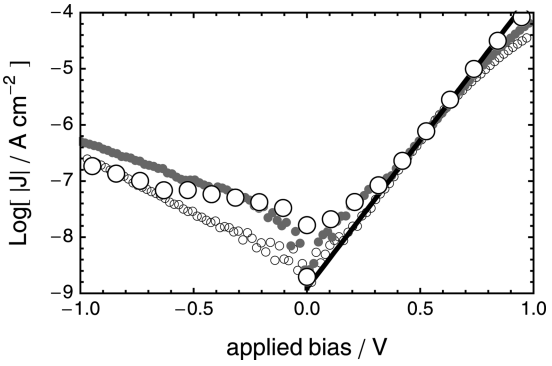

Figure 7. Current density (J) − applied bias (V_{app}) data for three separately fabricated PMEC p−n junctions. The large open circles are for the same junction as in Figure 3. The small open circles are for a junction with a 430 nm thick PA_A layer and 170 nm thick PA_C layer. The small solid circles are for a junction with a 360 nm thick PA_A layer and 400 nm thick PA_C layer. The solid line is an exponential fit with $n = 3.1$.

characterized by $n = 3.1$. The current density data for the three diodes are similar in this strong forward bias voltage range, and with the other two diodes being characterized by $n = 3.1$ and 3.5.

The J-V_{app} behavior of the p−n junctions exhibits two common deviations from ideal diode behavior. The first is the inevitable deviation from exponential at large forward bias due the finite resistance of the materials and leads; this series resistance results in the downward curvature of the log $J - V_{app}$ data near $V_{app} = 1$ V. The second is the presence of an apparent electrical shunt that prevents the reverse current from saturating and that is also consistent with the positive deviation in J from the exponential fit line in the forward bias voltage range $0.1 < V_{app} < 0.3$ V. The origin of this shunt appears to be related to imperfections in fabrication, as the reverse bias behavior is not as reproducible as the forward bias behavior.

Comparison of diode quality to junctions fabricated using other trapping approaches is somewhat challenging because of differences in materials, electrode geometry, and electrode materials. Nearly all reports have focused on luminescent polymers with higher band gaps than the nonluminescent polyacetylene materials studied herein. Furthermore, often only limited information on the J-V_{app} behavior is reported due to the emphasis on light emission. A commonly reported figure of merit is the rectification ratio (R), which is the ratio of the forward to the reverse current at a particular voltage. The rectification ratio for the PMEC fabricated polyacetylene junctions herein was found to maximize in the range of $V_{app} = 1-1.3$ with values as high as 900 being observed. Yu et al.[5] report rectification ratios in the range $10^4 - 10^5$ at 4 V for a frozen junction based on a poly(phenylene vinylene) derivative and using dissimilar ITO/Al electrodes, which introduces an additional source of asymmetry. Due to series resistance, it was not possible to accurately characterize the rectification ratio of the p−n junction fabricated herein at comparably high voltages. In the ideal case, the rectification ratio increases exponentially with voltage ($R = \mathrm{Exp}[V\beta n^{-1}]$), but it is often limited by either the series resistance or imperfections leading to electrical shunts. Inspection of the J-V_{app} data reported by Yu et al.[5] for the frozen junction based on the poly(phenylene vinylene) derivative shows nearly symmetric behavior ($R \approx 1$) out to 2 V and $n \approx 5.5$ in the range of $V_{app} = 2.5-3.5$ V where exponential behavior is observed. For junctions fabricated with the ion-pair monomer approach, rectification ratios in the range of 100−900 at 4 V have been reported for structures based on polyfluorene and/or poly(phenylene vinylene) using Au/ITO electrodes.[7]

The diode quality observed with the PMEC approach could not be achieved with the electrochemical disproportionation and trapping approach (EDAT) we previously reported.[12] In this previous report, EDAT was used to fabricated a p−n junction from ion-functionalized polyacetylenes with similar anionic and cationic functional group densities. The rectification ratio for the EDAT fabricated junctions near 1 V was nearly a factor of 100 less than reported here. For more direct comparison, an undoped bilayer consisting of the same polymers used herein was subjected to the EDAT approach. The resulting junction was more poorly conductive than the PMEC fabricated junction and had a rectification ratio of less than 5 at 1 V.

Conclusions

The use of the PMEC technique to fabricate internally compensated conjugated polymer p−n junctions was demonstrated. The PMEC fabricated p−n junctions exhibited diode behavior and a photovoltaic effect, with ideality factors in the range of 3−3.5 and rectification ratios as high as 900 near 1 V. PMEC is an effective tool for selectively doping regions of an ion-functionalized conjugated polymer structure. It also allows for the n- and p-type sides of the junction to be doped to differing extents, which is not possible with previously developed trapping approaches. The control of doping chemistry in this manner expands the range of electronic and photonic device architectures possible with conjugated polymers.

Acknowledgment. This work was funded by the Division of Chemical Sciences, Geosciences, and Biosciences, Office of Basic Energy Sciences of the U.S. Department of Energy through Grant DE-FG02-07ER15907. This project made use of equipment in the SUNRISE Photovoltaic Laboratory supported by the Oregon Built Environment and Sustainable Technologies (BEST) signature research center.